Focus Stacking with photogrammetry: An effective workflow for capturing sub-millimeter detail in the photogrammetric digitization of Roman coins.

ADAM REDFORD, Bournemouth University, UK
EIKE ANDERSON, Bournemouth University, UK

Conventional photogrammetric methods often struggle with the fine details and delicate features of ancient coins, which are critical for numismatic analysis. This paper presents an effective workflow integrating focus stacking with photogrammetry to enhance the digitization of Roman coins, achieving high-quality sub-millimeter detail. Focus stacking, which combines multiple images taken at different focus points into a single image with extended depth of field, addresses this limitation. By systematically capturing and processing stacked images, our workflow significantly improves the depth and clarity of surface details. We evaluate the workflow's efficacy through a comparative analysis against established photogrammetric techniques, highlighting substantial improvements in the quality of 3D models and textures. The research includes a step-by-step guide, from image acquisition using varied focal planes to the integration and processing within photogrammetric software. Results demonstrate that our workflow not only preserves the minute features of Roman coins but also facilitates better visual and qualitative analysis for researchers and curators. This advancement paves the way for more detailed and accurate digital representations of numismatic artifacts, contributing to enhanced documentation, study, and preservation of cultural heritage.

Keywords:
Photogrammetry, sub-millimeter, focus-stacking, Roman coins, numismatics.

SDH Reference:
Redford, Adam, and Eike Anderson. 2025. "Focus Stacking with photogrammetry: An effective workflow for capturing sub-millimeter detail in the photogrammetric digitization of Roman coins." Studies in Digital Heritage 9 (2): 196–228.

https://doi.org/10.14434/sdh.v9i2.40583

1. INTRODUCTION

In recent years, mainly due to improvements in the availability and affordability of relevant hardware and software, digital photogrammetry has gained popularity as a technique employed in archaeology and cultural heritage, providing an effective means for the documentation and analysis of artifacts and historical sites. This technique, which involves the use of photographs to create precise 3D

Author's address: Adam Redford, National Centre for Computer Animation, Bournemouth University, Fern Barrow, Poole, Dorset, UK, BH12 5BB; email: aredford@bournemouth.ac.uk; Eike Anderson, National Centre for Computer Animation, Bournemouth University, Fern Barrow, Poole, Dorset, UK, BH12 5BB; email: eanderson@bournemouth.ac.uk

models, has been instrumental in preserving invaluable archaeological findings and making them accessible to a broader audience. Among the many artifacts that benefit from photogrammetric techniques, Roman coins stand out due to their intricate designs and historical significance. However, capturing the sub-millimeter details of these ancient coins presents significant challenges that require sophisticated methods to overcome.

The importance of capturing sub-millimeter detail in ancient coins cannot be overstated. These coins are not merely currency; they are artifacts that offer rich insights into the socio-economic conditions, political history, artistic endeavors of ancient Rome, and last, but not least, provide dating evidence to archaeological finds (Kemmers and Myrberg 2011; Tolksdorf et al. 2017). Each coin carries unique features such as inscriptions, symbols, and portraits that can be as small as a few micrometers. Accurately identifying and documenting these details is crucial for numismatists, historians, and archaeologists who rely on this information to understand the past and preserve it for future generations.

Despite the advancements in photogrammetry, capturing sub-millimeter detail with this technique remains a formidable challenge. The primary issue lies in the inherent limitations of photogrammetric processes when dealing with objects that have fine, intricate details. Conventional photogrammetry can struggle to capture the subtle nuances of a Roman coin's surface, resulting in 3D models that lack the necessary quality. This limitation hinders detailed analysis and can lead to incomplete or misleading interpretations of the coin's historical and cultural significance. We aim to address the shortcomings of conventional approaches by combining the use of a medium format camera equipped with a zoom lens, a close-up lens, and a polarizing filter with focus stacking.

This article is structured as follows: in section 2 we present an overview of previous and related work, followed by a description of the Roman coins that we used in this project in section 3. In section 4 we provide an overview of the photogrammetry equipment that we employed, including both hardware and software used. We then describe our digitization workflow in detail in section 5, starting from the setup of the object to be digitized and the camera, via image acquisition and post-processing to the final generation of the 3D models using photogrammetry software. This is then followed by the presentation, analysis, and discussion of our results in section 6. Finally, in section 7 we draw conclusions from the project and present an outlook on future work.

2. FOCUS STACKING AND PHOTOGRAMMETRY FOR CAPTURING MICRO-SCALE OBJECTS

Over the years, different approaches for 3D capturing of very small objects with fine details have been employed in the analysis of archaeological finds, such as Roman coins, which have frequently been the subject of these studies. Schirripa Spagnolo et al. (2003) proposed the use of conoscopic holography for acquiring 3D models, combined with high-resolution 2D photographs to provide color information. Zambanini et al. (2009; 2010), Kampel et al. (2009), as well as Tolksdorf et al. (2017) employed multi-view (stereo) fringe projection systems, a technology related to structured light 3D scanners, that combine a single light projector with two cameras to capture 3D objects. Using a related approach but aiming for a low-cost solution, Schirripa Spagnolo et al. (2021) presented a simple single-view fringe projection system, combining a light projector with a single camera, which is

limited to creating one-sided 2.5D models of coins. More recently, Abate et al. (2024) employed X-ray computed microtomography to 3D scan and 'virtually clean' encrusted and corroded Roman copper coins.

Bentkowska-Kafel et al. (2016; 2018) investigated several different approaches to 3D scanning of Roman coins, including SfM (Structure from Motion) photogrammetry and focus stacking, to compare the effectiveness of these approaches and to identify how these might be combined or complement one another. One such combination of techniques was explored by MacDonald et al. (2017), integrating a photometric image set of a Roman coin with the point cloud resulting from a 3D color laser scan of the coin to obtain more accurate surface details. Detailed analytic comparisons and discussions of different techniques for digitizing heritage objects have been presented by Brecko and Mathys (2020), as well as by Adamopoulos et al. (2021).

3D heritage objects created using photogrammetry compare favorably with those created by other techniques (García-Bustos et al. 2024). Furthermore, many of the applied techniques and technologies, unlike many photogrammetry-based approaches, require the use of very expensive equipment, such as X-ray machines (e.g. for computed microtomography) or laser scanners. As a result, in recent years, close-range photogrammetry using DSLR (Digital Single-Lens Reflex) cameras has become the prevalent technique for digitizing small and micro-scale archeological objects (Hernández-Muñoz 2023).

Gillies (Gillies 2015) provided a brief and anecdotal historical overview of close-range photogrammetry, discussing its origins that pre-date the advent of digital cameras. Sometimes also referred to as macro photogrammetry (Gajski et al. 2016), the process of close-range photogrammetry was reviewed and discussed in some detail by Galantucci et al. (Galantucci et al. 2018), who investigated different approaches, as well as related aspects of this image-based 3D scanning method, with other studies focusing specifically on some of these aspects, such as camera calibration (Percoco et al. 2017) or the overlap of source images (Guidi et al. 2020). Gallo et al. (2014) and Gajski et al. (Gajski et al. 2016) explored the application of close-range photogrammetry in archeological contexts.

When dealing with sub-millimeter details on very small objects, digital microscopes can be used as an inexpensive alternative to DSLR cameras (Antinozzi et al. 2022), offering a high level of magnification and detail in small areas, although the overall image resolution of these devices is limited, requiring a large number of images to provide sufficient coverage. In recent years, several studies have compared the results of 3D heritage models that were generated using photogrammetry with those created by other 3D scanning approaches, such as structured light scanning (Polo et al. 2022) or X-ray computed microtomography (Scaggion et al. 2022), generally finding that photogrammetry, if competently carried out, results in 3D models of a good quality compared to other techniques, as already mentioned above, with all techniques having both strengths as well as weaknesses.

One of the factors that has been identified to determine the quality (e.g. mesh density, average edge length, texture resolution, etc.) of 3D models created using photogrammetry is the quality of the source images (O'Connor 2018), which to a large extent itself depends on the quality and capability of

the used camera, as can be seen, e.g. in the work by Saif and Alshibani (2022), who compared photogrammetry 3D models created using a DSLR camera with those resulting from the use of a smartphone. A possible approach to improving source image quality is to use a camera with built-in pixel-shift functionality to create highly detailed super-resolution images (D'Urso and Aldrighettoni 2024). Source image quality also depends on the acquisition process, where, e.g., a lack of care during image acquisition (Polo et al. 2022) or the use of a hand-held camera, as opposed to a camera being mounted on a tripod, can have a negative influence on the quality of the resulting 3D model (Barszcz et al. 2021). A detailed discussion of the factors that influence the results of 3D capture of objects using photogrammetry has been provided by Mosbrucker et al. (2017), including image quality, camera system selection, and the photogrammetry software used. Comparisons and analyses of the latter's influence on the resulting 3D models were carried out by Kingsland (2020), Đuric et al. (2021), and Piazza et al. (2024).

Existing 3D models of Roman coins generated through photogrammetry (Hess et al. 2018; Morris et al. 2022) often fall short in capturing the minute details that are essential for comprehensive study. The limitations of these models are primarily due to the difficulty in obtaining sharp, high-quality images of the coin's surface. The conventional approach involves taking multiple photographs from different angles and then using photogrammetry software to create a textured 3D model (Dey 2018). However, even slight imperfections or perturbations in the images, particularly when dealing with objects that require sub-millimeter detail such as carved gemstones (Gołyźniak 2020), fine metalwork (Armbruster 2023), or small-scale modifications to bones or teeth (DeSantis et al. 2013), can lead to significant loss of detail in the resulting 3D model (Stamatopoulos et al. 2012).

To address these challenges, the focus stacking process has been introduced as a potential solution (Gallo et al. 2012; 2014; Kontogianni et al. 2017; Galantucci et al. 2018), where these early attempts used cameras that did not provide any automation for this effect, requiring additional processing with extensive calculations. Focus stacking involves taking several photographs of the same object at different focal distances and then combining them to produce a single image with a greater depth of field. Although this technique has sometimes been dismissed as unsuitable for photogrammetry (Historic England 2017), Gallo et al. (2014), as well as Plisson and Zotkina (2015) showed that it can be successfully combined with photogrammetry, where it is particularly useful for capturing the fine details of small objects, such as Roman coins, and where the depth of field in a single photograph is often insufficient. More recently, focus stacking photogrammetry has been shown to result in 3D models that can rival those created using X-ray computed microtomography (Brecko and Mathys 2020). That said, however, the focus stacking process can be quite laborious and time-consuming if not handled correctly or if the hardware used does not fully support this. It requires careful planning, precise control of the camera, and meticulous post-processing to ensure that the combined images accurately represent the photographed object's surface. For example, Clini et al. (2016) used a full-frame camera that did not support automatic focus bracketing, the process of fixing the position of the camera and systematically changing the focus plane of the lens until all parts of the object have been captured in-focus and an essential part of the focus stacking process, thereby making it necessary to add an additional processing step to the digitization of archaeological artifacts. This type of hardware limitation, requiring additional processing steps, is quite common (Kontogianni et al.

2017; Ravanelli et al. 2022). A similar process is the one described by Olkowicz et al. (2019), who did not employ any focus bracketing, which is not true focus stacking, but which could more accurately be referred to as a type of 'focus isolation'.

In any case, planning, image acquisition, post-processing, and other supporting activities are usually formalized in photogrammetry workflows, such as those described by Marziali and Dionisio (2017), Historic England (2017), or Redford et al. (2020)—some of which also incorporate focus stacking (Ravanelli et al. 2022). The workflow employed by the latter, similar to that by (Lastilla et al. 2021), also included the use of the photogrammetry software's 'import masks from model' parameter for generating the image masks prior to alignment, which is more efficient and tends to provide better results than workflows that instead employ dense point clouds, which used to be the norm (Clini et al. 2016).

Given the labor-intensive nature of focus stacking, there is a clear need for the automation of certain parts of the workflow, as well as the efficient batch processing of large data-sets, which our workflow implements. Automation can significantly reduce the time and effort required to capture and process the images, making the workflow more efficient and less prone to human error. Similarly, batch processing allows for the automated processing of multiple images, further streamlining the workflow. Together, these advancements can make the focus stacking process more practical for large-scale projects, where the manual handling of each image would be impractical.

3. THE COINS

Fig. 1 depicts the four Roman coins from the first author's personal collection that were used for this project.

Coin 001 is a badly damaged (most of the edge, including the inscription on the obverse and the exergue with the mintmark on the reverse are broken off) bronze nummus (AE3) (Mattingly 1946), featuring the right-facing pearl-diademed bust of the Roman emperor Constantius II (337–361 AD), a son of emperor Constantine I ("Constantine the Great") and his wife Fausta (a daughter of emperor Maximian – see coin 003) on its obverse (Frakes 2005). The legend is almost completely missing, with just the bottom half of an 'A' remaining, but would have read "[D N CONSTANTIVS P F]A[VG]" ("Dominus Noster Constantius Pius Felix Augustus", i.e. "Our lord Constantius, the pious and blessed emperor"). The reverse shows a wreath within which parts of the inscription "VOT XX [MVLT] XXX" ("Votis Vicennalibus Multis Tricennalibus", i.e. "(prayers) on the twentieth anniversary (of the emperor's rule) and more (wishes) for his thirtieth anniversary") (Stevenson et al. 1889), the top two and the last of the originally four lines are still decipherable. The mintmark is missing, but the coin was issued around 20 years after Constantius was elevated to the position of Caesar (324 AD) and most likely dates to 345–350 AD.

Figure 1. The four Roman Coins used for this project.

Coin 002 is a bronze nummus (most likely AE3), issued by the Roman emperor Constantine I, the obverse bearing the legend "FL IVL CONSTANTIVS NOB C" ("Flavius Iulius Constantius Nobilissimus Caesar") and depicting a laureate, cuirassed, and right-facing bust of his son, the teenage prince Constantius, who would succeed his father as 'Augustus' in 337 AD (see coin 001). The reverse of the coin features two standing helmeted, draped, and cuirassed soldiers, facing each other with each holding a reversed spear in their outer hand and resting their inner hand on a shield, flanking two standards that are standing between them (Bruun 1997). The partially faded but still complete inscription of the reverse is "CLOR IA EXERC ITVS" ("gloria exercitus", i.e. "the glory of the army") (Stevenson et al. 1889). The coin was minted in Lugdunum (mintmark "PLC", now Lyon in France), with the mintmark preceded by a dot (series mark), dating the coin to ca. 330–331 AD.

Coin 003 is a bronze post-reform radiate (Bruun 1979) (Neo-Antoninianus (Kropff 2017)), portraying the bust of Roman emperor Maximian (Marcus Aurelius Valerius Maximianus, co-emperor of emperor Diocletian from 286–305 AD (Frakes 2005)), cuirassed, facing right with a radiate crown and featuring the legend "IMP C M A MAXIMIANVS P F AVG" ("Imperator Caesar Marcus Aurelius

Maximianus Pius Felix Augustus") on the obverse. The reverse of the coin depicts the prince standing on the right and receiving a small Victory on a globe from Jupiter, standing on the left and leaning on a scepter with his left hand, accompanied with the inscription "CONCORDIA MILI TVM" ("concordia militum", i.e. "in harmony with the soldiers"). The coin was struck in the 4th (mark 'delta') officina (workshop) of the mint at Heraclea (established in 291 AD in the old Greek city of Perinthos, now Marmara Ereglisi in the European part of modern Turkey, with the mintmark 'H') and dates to the early years of the Tetrarchy around 295–296 AD.

Finally, coin 004 is an Antoninianus from the height of the Roman empire's 'crisis of the third century' (Nicols 2007) with the bust of the emperor Gallienus (260–268 AD), cuirassed, and facing right with a radiate crown on the obverse. The majority of the legend is missing, leaving fragments of the inscription "[GALLI]ENVS AVG" ("Gallienus Augustus"). The coin's reverse depicts the goddess Pax (peace), draped and standing, facing left, holding a palm or olive branch in her right hand and a long transverse scepter in her left hand, with the fragmentary inscription "PAX AE[TERNA A]VG" ("pax aeterna Augusta", i.e. "everlasting peace of the emperor"). The left field also shows the officina letter delta, but no other mintmark is decipherable (similar coins were minted in Rome).

4. EQUIPMENT

4.1 Photography Equipment

4.1.1 Camera and Lens

For this project, we utilized the Fujifilm GFX100s, a mirrorless medium format camera renowned for its exceptional resolution and advanced functionality. The GFX100s offers two key advantages that significantly enhanced the quality of our work. First, its sensor, larger than a full-frame sensor and measuring 43.8mm x 32.9mm, allows for an image resolution of up to 11648 x 8736 pixels. This resolution provides a high level of detail, surpassing that of cameras with smaller sensors, such as full-frame sensors (35mm x 24mm) or APS-C sensors (25.1mm by 16.7mm), with an additional benefit provided by the larger sensor being noise reduction (Cao et al. 2010). Second, the camera's ability to perform automated focus bracketing proved invaluable. Automating the process of shooting the focus brackets is essential in reducing the amount of time it takes to photograph each coin.

The lens used in this project was the Fujinon GF35-70mm zoom lens. To further enhance the level of detail captured, we attached a circular polarizing filter and a Nisi close-up lens. The circular polarizing filter reduced any reflected light from the surface of each coin, while the close-up lens reduced the minimum working distance of the camera from 35cm to 22cm, allowing us to move closer to the subject and capture even finer details. This proximity, combined with the camera's high resolution and focus bracketing functionality, enabled us to capture images of an exceptional level of detail, which was critical for the success of this project.

Finally, the camera was connected to an external monitor via an HDMI cable to allow for easier viewing, framing, and focusing of the coins without the need to look through the camera's integrated viewfinder.

4.1.2 Tripod and Turntable

For this project, we used the Manfrotto 055 tripod paired with a MHXPRO-3W head, providing a stable and highly adjustable platform for our camera setup. The Manfrotto 055 is known for its durability and versatility, making it an excellent choice for precise photography work. The MHXPRO-3W head, with its three-way pan-and-tilt mechanism, allowed us to fine-tune the camera's positioning, ensuring consistent framing throughout the shoot.

To achieve precise rotational control for our images, we used the Foldio 360 Smart Turntable, a tool designed to automate and streamline the process of capturing 360-degree product images. The turntable was connected to an iPhone 14 Pro, enabling remote activation and control via a dedicated app. This integration of the smart turntable with the iPhone allowed us to precisely dictate the degree of rotation between each set of photographs, ensuring uniformity in our captures. The turntable was programmed to rotate in 8-degree increments, resulting in a total of 45 sets of stacked photographs to cover the full 360-degree rotation. This method ensured that each angle was captured, facilitating the creation of a seamless and comprehensive 360-degree view of each coin.

4.1.3 Lighting

Lighting was a critical component of this project, as achieving consistent and soft illumination was essential to minimizing shadows and capturing each coin with clarity. To ensure uniform lighting, we utilized a custom-made light box, specifically designed to produce an even distribution of light around the subject. The light box featured three large 60cm LED panels, each emitting light at a color temperature of 5600K. The floor and backdrop of the light rig were covered in white paper in order to provide as much indirect illumination to the scene as possible. This setup provided a broad, soft light source that helped to eliminate harsh shadows and create a balanced lighting environment. Additionally, we supplemented this with two smaller Neewer LED light panels positioned at the front of the light box, also set to 5600K. These additional lights enhanced the overall illumination, ensuring that the coin being photographed was evenly lit from all angles. This comprehensive light rig setup, as shown in Fig. 2, not only allowed us to achieve the desired lighting conditions but also enabled us to use a faster shutter speed on the camera. By increasing the amount of light on the subject, we were able to reduce the risk of motion blur, which is a common issue when using slower shutter speeds due to insufficient lighting. This precise control over the lighting environment was crucial in capturing sharp, high-quality images with minimal noise and distortion.

Figure 2. The light rig setup showing the three 60cm LED light panels and two smaller front LED light panels.

4.1.4 Other Photography Accessories

In addition to the primary equipment, we utilized several key accessories to enhance the efficiency and quality of our work. A tripod dolly was employed to facilitate easier movement of the tripod, allowing us to reposition the camera smoothly and without disturbing the setup. This was particularly useful when slight adjustments were needed to achieve the perfect angle or composition.

To further minimize the risk of camera-shake and ensure the highest image quality, we used a wireless remote shutter release. This tool allowed us to trigger the camera without physically touching it, thereby reducing the possibility of vibrations that could lead to blurred images. This was especially important given the extremely close focus distance of the camera, where even the slightest movement could impact the sharpness of the final images.

For accurate color calibration, we incorporated an X-Rite ColorChecker Classic into the workflow. This color calibration tool is essential for ensuring that the colors captured in the images are true to life and consistent across different coins. By including the ColorChecker in our process, we were able to achieve precise color reproduction, which is crucial during post-processing and when generating the final textures during the photogrammetry process.

4.2 Computer Equipment

4.2.1 Hardware

The computer hardware used for this project was carefully selected to handle the demanding processing requirements of photogrammetry, and the rendering of textured 3D models. The system was built around a powerful PC equipped with an Intel Xeon W-2255 CPU, running at 3.70GHz, and 32GB of internal system ram. This high-performance processor provided the necessary computing power to efficiently handle complex tasks such as image processing, rendering, and data management.

Complementing the CPU was an Nvidia RTX A5500 graphics card, featuring 24GB of GDDR6 memory. This GPU was essential for accelerating tasks that involve heavy graphical computation, such as photogrammetry, and rendering high-quality images from 3D scenes containing large amounts of geometry and texture data. The large memory capacity of the graphics card ensured that even the most demanding GPU dependent tasks could be executed smoothly, without bottlenecks.

Storage needs were met with a 1TB SSD, offering both speed and capacity. The SSD allowed for rapid access to large image files, reducing loading and processing times, which is critical when working with large amounts of data. This storage solution also provided ample space for managing multiple projects and backups, ensuring that all data was securely stored and easily accessible.

To streamline the workflow, the machine was also equipped with an integrated SD card reader. This feature facilitated the quick and easy transfer of image files from the camera to the computer, eliminating the need for external adapters and reducing the time spent on file management. Overall, this robust hardware setup ensured that the project could be executed efficiently, with the computing power necessary to maintain high standards of quality throughout the process.

4.2.2 Software

The software suite used for this project was carefully chosen to handle various aspects of the workflow, from initial image processing to final rendering. The system operated on Windows 10, a reliable and versatile operating system that provided a stable foundation for running the required software applications.

Adobe Camera Raw played a crucial role in the initial stages of image processing. This software was used for essential tasks such as white balancing, exposure correction, and brightness adjustments. By processing the image files, Adobe Camera Raw ensured that the images maintained their highest possible quality before moving on to the focus stacking and photogrammetry stages of the pipeline.

For focus stacking, we utilized Helicon Focus version 8. This software was indispensable for combining multiple images taken at different focus points into a single image with an extended depth of field. Helicon Focus allowed us to create sharp, detailed images by seamlessly blending these layers, which is particularly important in macro photography.

Agisoft Metashape Pro version 2.0.2 was employed for the photogrammetry work. This advanced software is renowned for its ability to generate 3D models from 2D images by reconstructing the spatial geometry of the photographed subject. It enabled us to create highly accurate and detailed 3D models, which were essential for the project's objectives.

Finally, Autodesk Maya version 2023, in conjunction with Arnold version 7.2 renderer, was used for the final image rendering. Maya, a leading 3D modeling and animation software, allowed us to refine the 3D models and prepare them for rendering. Arnold, the powerful rendering engine integrated within Maya, was then used to produce the final high-quality images. Arnold's advanced GPU rendering capabilities ensured that the final outputs were not only visually stunning but also met the high standards required for the project.

5. WORKFLOW PROCESS

5.1 Photography

5.1.1 Object Setup

The first step in the object setup process is ensuring that the coin being photographed is precisely centered on the turntable. If the coin is not accurately positioned at the exact center, it can lead to complications during the photography process. As the turntable rotates, any misalignment requires continuous adjustments to the camera angle, which not only increases the time needed to photograph each coin but may also necessitate frequent recalibration of the focus bracketing settings. To determine the exact center of the circular turntable, a method involving geometric principles was used. Three equal-length lines (chords) were drawn along the outer edge of the circle. From the midpoint of each chord, a perpendicular line was extended toward the interior of the circle. The point where these perpendicular lines intersected marked the exact center of the turntable, as illustrated in Fig. 3. This method ensured a precise central reference point for positioning the coin.

Figure 3. Turntable with exact center marked by intersecting right-angle lines.

Once the center was identified, the coin to be photographed was carefully placed on a small rubber support located at the turntable's center. The rubber support not only helped to stabilize the coin but also allowed for minor adjustments to ensure perfect alignment. To enable object scaling during the photogrammetry process, three sets of printed markers for coded target recognition were added to the side of the rubber support, as shown in Fig. 4. These markers played a critical role in ensuring that the scale and alignment of the images were consistent throughout the capture process. By carefully centering the coin and using coded markers, we were able to streamline the photography process, reduce the need for continuous adjustments, and ensure that the images captured were of the highest possible quality. The scale markers were accurately measured using a pair of digital calipers as shown in Fig. 5.

Figure 4. Coin placement (coin 003) showing the rubber support and three sets of printed markers for scaling

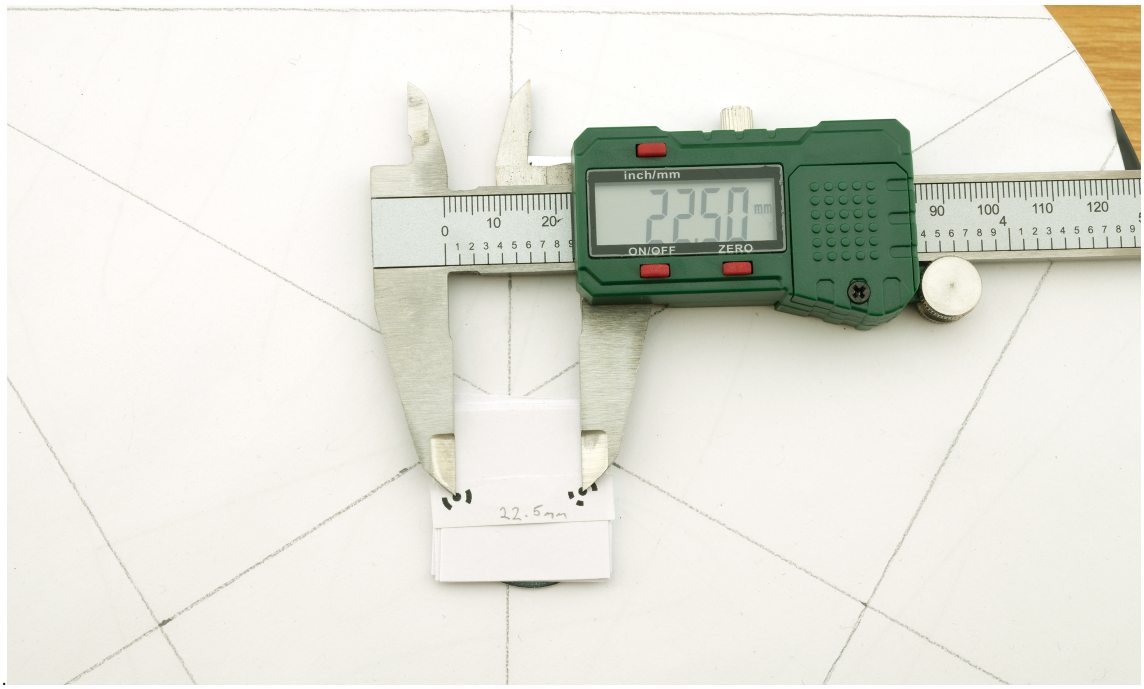

Figure 5: The accurate measurement of the scale markers using a pair of digital calipers.

5.1.2 Camera Settings

The camera's aperture was set to f/22. Although this setting is slightly narrower than the optimum aperture value of f/11, it was chosen for its balance between depth of field and image sharpness. The minimum possible aperture for the lens, f/32, would have increased the depth of field, but it would also have introduced significant blurring due to lens diffraction. This blurring could have compromised the quality of the final photogrammetric construction of the 3D model and its texture, leading to suboptimal results. Using the optimum aperture value of f/11 would have required a significantly higher number of focus-bracketed images to achieve full focus coverage of each coin—approximately twice as many images. For instance, coin number 001 required 31 bracketed images at f/22, a total of 2790 images, to achieve full focus coverage. In contrast, if shot at f/11, the same coin would have necessitated 63 bracketed exposures, a total of 5670 images. Thus, f/22 was determined to be the most efficient choice, balancing the need for sharpness and depth of field while minimizing the number of images required.

The focal length of the lens was set to the maximum of 70mm, which, when compensating for the image sensor's crop factor, gives a full-frame equivalent focal length of 55.3mm. The camera's ISO was set to 100 to maintain image quality with minimal noise, and the shutter speed was 1/2.5th of a second, providing the necessary exposure at the correct brightness according to the camera's in-built light meter. The white balance was carefully matched to the color temperature of the LED light panels in the light rig, which was set at 5600 Kelvin, ensuring accurate color reproduction in the captured images.

Due to the large file sizes associated with the camera's native raw format, it was decided to use JPEG as the image file type. While raw images offer greater flexibility in post-processing, the substantial increase in file size would have made managing the data sets for each coin impractical. For example, the image set for coin 001 amounted to approximately 92GB when using JPEG, whereas the size would have increased to approximately 556GB if shot in raw format. This decision was crucial in keeping the project data manageable without significantly compromising image quality (Falkingham 2020).

Focus bracketing was handled automatically by the camera, which was first configured to set the nearest and farthest points of focus. This automation ensured consistent focus coverage across the entire surface of each coin, further streamlining the process and contributing to the overall efficiency of the project.

5.1.3 Image Acquisition

The process of capturing the images for each coin was streamlined and efficient, thanks to the combined use of the wireless remote and the app-controlled smart turntable. After taking a single photograph of the X-Rite ColourChecker Classic chart for color calibration purposes, and adjusting the camera's exposure compensation function accordingly, the turntable was programmed to rotate in 8-degree increments, requiring 45 rotations to cover the 360 degrees necessary for full subject coverage. At each incremental rotation, the camera's shutter was activated remotely using the wireless remote. Once the shutter was triggered, the camera's internal software automatically initiated the focus bracketing process, capturing a series of images at different focus points based on the previously determined nearest and furthest focal distances. The coin was then turned over to

capture the same set of images of the bottom half of the coin, with the intention of combining the two halves at a later stage in the workflow process.

This semi-automated approach not only simplified the task of photographing each coin but also ensured that every angle and detail was captured with consistency.

5.2 Post-processing

After the image acquisition stage, the next step was to process the images to prepare them for the photogrammetry stage. Adobe Camera Raw, in conjunction with the X-Rite ColorChecker Classic chart, was utilized to carry out the post-processing tasks. This stage involved minor adjustments, including ensuring that the images were correctly white-balanced, removing any chromatic aberration, and applying slight sharpening when necessary. These adjustments were crucial for maintaining consistency and quality across the entire set of images.

Following the initial post-processing, it was necessary to organize the full set of photographs into sub-folders, with each folder containing a complete set of images corresponding to one of the 45 rotational positions captured. To streamline this organizational step, a simple PowerShell script was written to automate the process of moving the images into their respective folders (see Appendix 1). The script was designed to be user-friendly, requiring only three variables to be specified: the source directory containing the images, the destination directory where the folders would be created and the images moved to, and the number of images to be placed in each folder.

Once all the source images were organized into individual folders corresponding to each focus stack, we were able to batch-process the focus stacking stage. This was efficiently handled using the “Add multiple folders” option within Helicon Focus’s batch processing tool. This approach not only saved time but also ensured that the focus stacking was consistently applied across all images, laying a strong foundation for the subsequent photogrammetry work.

5.3 Photogrammetry

Following the completion of the post-processing and focus stacking stages, the next step was to generate fully textured models of each coin using Agisoft Metashape photogrammetry software. This process began with image alignment, aimed at creating a low-polygon mesh that would be used to generate image masks.

To produce the so-called “Masking Mesh” (Lastilla et al. 2021; Ravanelli et al. 2022) for each coin, the top and bottom image sets were first imported into Metashape and aligned in separate chunks. The "Align Photos" parameters within Metashape were configured for the Highest accuracy, with a Key Point Limit of 40,000 and a Tie Point Limit of 4,000. Once the image alignment was completed, a low-poly mesh was generated, with the Quality and Face Count parameters set to Medium. This mesh served as a preliminary model, and it was manually edited to remove any unwanted geometry, as shown in Fig. 6. Next, the image sets for each chunk were masked using Metashape’s "Generate Masks" function. The Method parameter was set to “From Model,” and the Apply To parameter was set to “All Images,” as illustrated in Fig. 7.

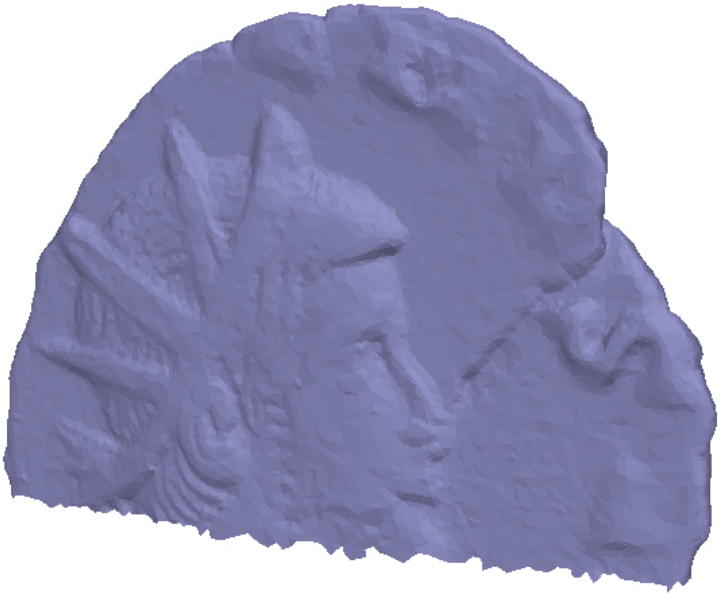

Figure 6. A low-polygon masking mesh of coin 004.

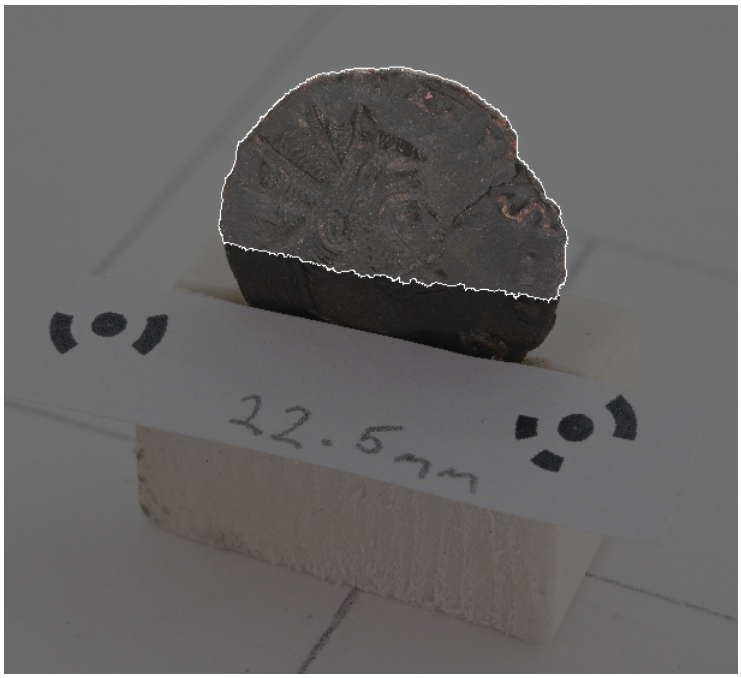

Figure 7. A single image from the Top chunk of coin 004 showing the mask generated by the masking mesh method.

After masking the images in both the top and bottom chunks using this masking mesh method, the masked images were combined into a new chunk containing all 90 images from the original top and bottom chunks. The image alignment process was then re-run on this newly combined chunk, with enhanced settings: an accuracy level of Highest, a Key Point Limit of 200,000, and a Tie Point Limit of 20,000. Additionally, the parameters for the "Align Photos" tool were configured to apply masks to key points, and the “Generic Preselection” option was disabled ensuring successful alignment of both halves of the coin together in a single chunk. Applying masks to the key points enables both the top and bottom photo sets to be aligned together, giving full coverage of the coin. The result of this full alignment of the combined chunk containing both top and bottom halves of the coin is depicted in Fig. 8.

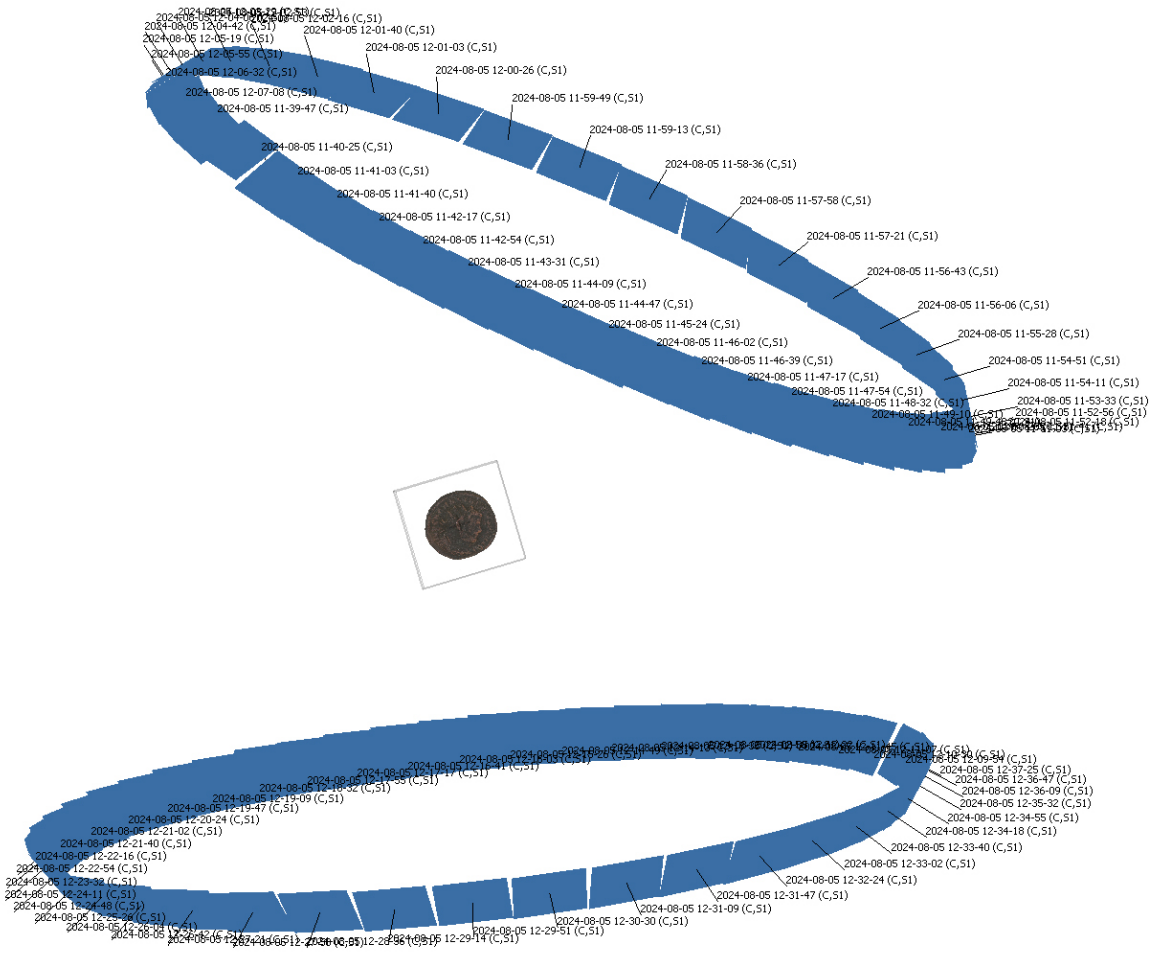

Figure 8. A screenshot showing the aligned cameras’ positions in Metashape.

Once all 90 images were aligned, a high-poly mesh was generated using the depth maps as the source data, with both the Quality and Face Count parameters set to High. Two 8k textures were then created for the coin, providing detailed surface representation. Finally, the model was accurately scaled using the "Detect Markers" and "Create Scale Bar" functions within Metashape, ensuring that the final 3D model was true to the coin's real-life physical dimensions, as shown in Fig. 13.

6. RESULTS ANALYSIS & COMPARISON

Our results show that combining focus stacking with photogrammetry, using an efficient and effective workflow such as the one demonstrated here, can produce highly detailed results that surpass the capabilities of conventional (i.e., basic) non-focus-stacked photogrammetric techniques.

6.1 Analysis of Focus Stacking Results

The resulting textured 3D models exhibit a high level of detail, enabling the production of high-quality beauty renders, as shown in Fig. 9. The focus stacking process ensures that each photograph used in the photogrammetric model is sharp and detailed, while the photogrammetric software stitches these images together to create a comprehensive textured 3D model. In Fig. 10 and Fig. 11, sub-millimeter details are clearly visible in the rendered images, demonstrating the detail achieved using our focus stacking methodology. The rendered images are each overlaid with a 1mm grid, further highlighting the fine details captured in the textured 3D models of each coin. The final textured 3D models have been uploaded to SketchFab and are accessible using the links in Appendix 2.

Figure 9. A beauty render of the final textured 3D models of the coins.

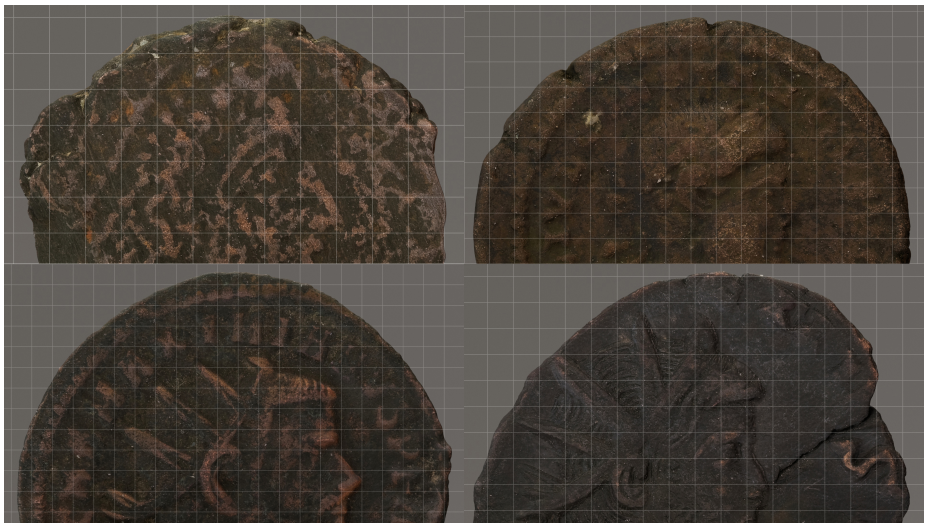

Figure 10. A close-up render of each textured 3D coin model with a 1mm grid overlay, clearly showing sub-millimeter detail (clockwise from the top: coins 001, 002, 004 and 003).

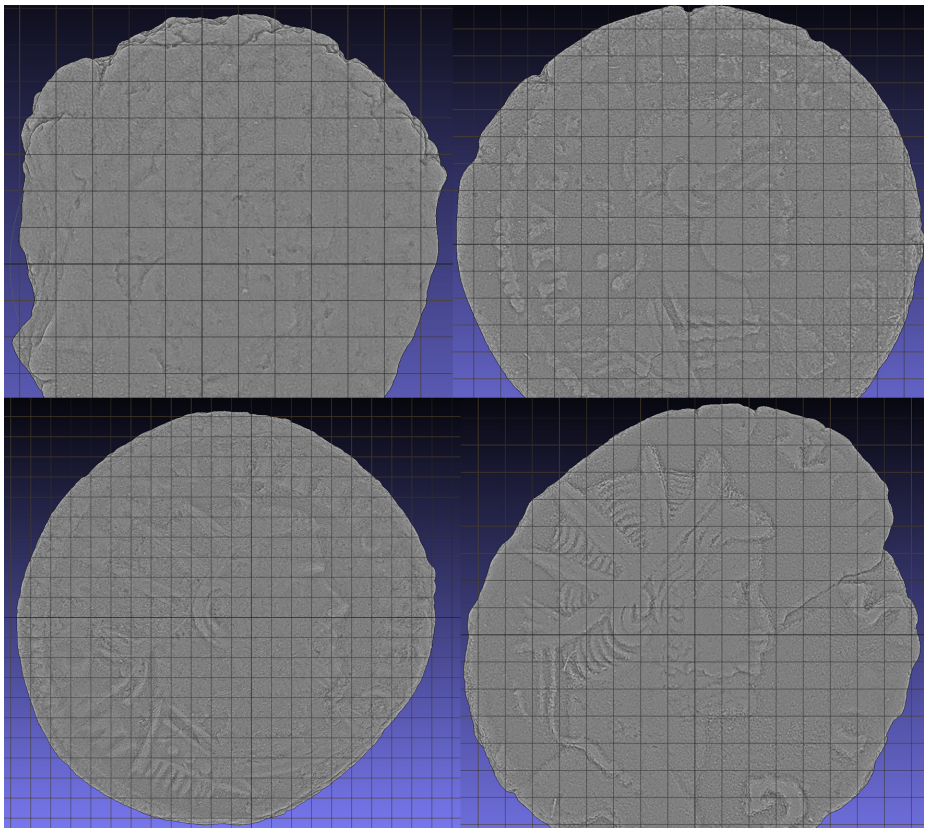

Figure 11. A close-up render, using MeshLab's Radiance Scaling shader, of each 3D coin model with a 1mm grid overlay, clearly showing sub-millimeter detail (clockwise from the top: coins 001, 002, 004 and 003).

6.2 Comparison with Other Methodologies

In analyzing the results of our methodology, we decided to conduct four distinct points of comparison to evaluate the effectiveness of our approach. The first point of comparison involved photographing the coins using the Fujifilm GFX100s camera's pixel shifting functionality, also known as Pixel Shift Multi Shot, to establish if the use of this technique might provide a viable alternative to focus-stacking. This feature enables the camera to take a series of 16 photographs with a single shutter release, shifting the camera's internal sensor by 1 pixel for each subsequent shot using in-body image stabilization (IBIS). The 16 images are then combined using specialized software to produce a single super-resolution image. The benefits of pixel shifting are twofold. First, it significantly increases the resolution of the final image, boosting it from 102 megapixels to approximately 408 megapixels. This increase in resolution enhances the level of detail captured, making it particularly beneficial for photogrammetry. Second, pixel shifting improves color accuracy by bypassing the standard demosaicing process, which interpolates color information from surrounding pixels. Instead, the sensor is shifted so that each pixel captures red, green, and blue data directly, resulting in more accurate and precise color representation in the final image, an additional side effect being reduced aliasing and moiré patterns (Qian et al. 2022). One of the main drawbacks of using the pixel shifting functionality is that it requires images to be captured in raw format, as JPEG compression is not supported. Consequently, the image dataset for a single coin—comprising 1,440 images—totaled approximately 135 gigabytes. This substantial increase in file size imposes higher demands on storage capacity, data transfer, and processing times. Additionally, pixel shifting shares similar challenges with focus stacking, particularly the need for both the camera and the subject to remain perfectly still throughout each capture sequence. Any movement during the sequence, whether from the camera or the subject, can result in misalignment and failure when attempting to combine the final images. This requirement makes the process highly sensitive to environmental conditions and equipment stability.

The second point of comparison involved generating a photogrammetric digitization using the same Fujifilm GFX100s camera and lens equipment but without employing focus stacking or pixel shifting. The third comparison used a camera with a full-frame sensor, again without focus stacking or pixel shifting, while the fourth comparison utilized a camera with an APS-C sensor, also without focus stacking or pixel shifting. These comparisons are aimed to more closely mimic equipment found in other research publications on photogrammetry for Roman coins and other small objects. We maintained consistency in other aspects of the process, including lighting, and the generation of the final 3D models and textures. For all four points of comparison, it was necessary to remove the close-up filter attached to the lens. The reason for this was that, on account of the extreme magnification provided by the close-up filter, the coin would not have been fully in focus even when using the lens's minimum aperture diameter, as shown in Fig. 12. It was also necessary to adjust the aperture setting from f/22 to f/29 when shooting with the GFX100s to ensure that the depth of field was wide enough for the whole coin to be in focus. Having a shallow depth of field with some areas of the coin out of focus would have compromised the comparison's validity by introducing variables unrelated to the focus stacking technique itself.

It was necessary to adapt our approach when capturing the full coin without focus-stacked images, as the Masking Mesh method proved ineffective in aligning the entire set of masked photographs. To

address this challenge, we employed a different method involving the generation of dense point clouds for both the top and bottom halves of each coin. Once the point clouds for each half were created, we used the "Align Chunks" and "Merge Chunks" functions in the photogrammetry software to accurately combine the two halves. After successfully merging the top and bottom point clouds, we were able to generate a mesh and texture for the complete coin.

Figure 12. The shallow depth of field encountered when using the close-up filter without the focus stacking method, showing that the foreground and background edges of coin 003 (highlighted) are out of focus when shot at an aperture value of f32.

This alternative approach allowed us to capture the full geometry and fine surface detail of each coin, overcoming the limitations of the Masking Mesh technique when applied to lower-detail, non-focus-stacked images.

The first and second comparison tests were conducted with the same FujiFilm GFX100s camera and lens setup that was utilized for the focus stacking method. For the third comparison, the camera used was a Canon 5D MkIII, which features a 35mm full-frame sensor. It was equipped with a 24-105 L-Series zoom lens which was zoomed to a focal length of 105mm. For the fourth comparison, we used a Canon 7D Mark II, which has an APS-C sensor. This was also equipped with the same 24-105 L-Series zoom lens set at 105mm focal length.

By using these five different setups, a detailed comparison can be found in table 1, we were able to rigorously test how sensor size, image number, and the absence of focus stacking influence the quality of the final 3D model (measurable e.g. using the average edge length in the generated 3D model—see table 2) and texture output, thus providing a comprehensive evaluation of our focus stacking methodology. This methodical approach allowed us to assess the specific impact of focus stacking on the level of detail achieved in the photogrammetric digitization process. By comparing our results with these more conventional methods and equipment, we could clearly quantify the

enhancement in detail and quality (e.g. smaller scale bar errors—see table 3) provided by our focus stacking methodology.

Table 1: A comparison of the five different setups used for coin 003.

	Setup 1	Setup 2	Setup 3	Setup 4	Setup 5
Sensor Type	Medium Format	Medium Format	Medium Format	Full Frame	APS-C
Lens Type	55-70mm Zoom	55-70mm Zoom	55-70mm Zoom	24-105mm Zoom	24-105mm Zoom
Camera Settings	ISO – 100 Shutter Speed – 1/2 Sec Aperture – f22	ISO – 100 Shutter Speed – 0.77 Sec Aperture - f29	ISO – 100 Shutter Speed – 0.6 Sec Aperture - f29	ISO – 100 Shutter Speed – 1/4 Sec Aperture - f22	ISO – 100 Shutter Speed – 1/3 Sec Aperture - f22
Photographic Accessories	Polarizing Filter, Close-up Lens	Polarizing Filter	Polarizing Filter	Polarizing Filter	Polarizing Filter
Software Processing Steps	White Balance C/A Removal Sharpening Focus Stack	White Balance C/A Removal Sharpening Pixel Shift	White Balance C/A Removal Sharpening	White Balance C/A Removal Sharpening	White Balance C/A Removal Sharpening
Number and type of Scale Bars	3 Control	3 Control	3 Control	3 Control	3 Control
Focus Stacking Used	Yes	No	No	No	No
Pixel Shifting Used	No	Yes	No	No	No
Masking Mesh or Point Cloud	Masking Mesh	Point Cloud	Point Cloud	Point Cloud	Point Cloud
Approximate Total Time for Image Acquisition	48 Minutes and 30 seconds	24 Minutes and 15 seconds	5 Minutes and 44 seconds	5 Minutes and 47 seconds	5 Minutes and 46 seconds
Approximate Total Time for Image Processing	3 hours 25 minutes and 27 seconds	1 hour 28 minutes and 51 seconds	3 minutes and 15 seconds	46 seconds	40 seconds
Approximate Total Time for 3D Model Generation	36 Minutes and 49 seconds	5 hours 34 minutes and 12 seconds	1 hour and 1 second	7 minutes and 46 seconds	9 minutes and 20 seconds
Approximate Data Volume Collected	116.1 GB	167.4 GB	2.83 GB	310 MB	372MB
Approximate Camera and lens Cost (June 2025)	$8028.00USD	$7921.00USD	$7921.00USD	$1354.00USD	$880.00USD

Fig. 13 shows a comparison of the physical measurement taken of coin 003, and the digital measurement of the resultant mesh of coin 003 created using our focus stacking method. The digital measurement was taken using Metashape's Ruler function. Both measurements show exactly 21.2mm.

Figure 13. A comparison of the physical and digital measurements of coin 003. Both measurements show 21.2mm

As shown in Fig. 14 through Fig. 21, as well as in Tables 2 and 3, our focus stacking methodology consistently produces results with a higher level of visible detail and quality across all four comparison tests. The results also show that the results of pixel shifting, while providing greater visible detail than those achieved by using non-focus-stacked photographs taken by the same camera, despite the much higher resolution of the generated source images, fall short of the results attained using focus stacking. This furthermore demonstrates that source image resolution is only one of the factors that determine the quality of 3D models obtained using photogrammetry and, on its own, is not the main contributor to the level of visible detail in the generated 3D model. Fig. 14 through 17 show a side-by-side comparison of the final textured 3D models, clearly demonstrating the enhanced detail and quality achieved with focus stacking. Similarly, Fig. 18 through Fig. 21 present a side-by-side comparison of the untextured geometry, further highlighting the improvements in surface detail and overall model fidelity when using our focus-stacking method.

Table 2: The average edge length (as a measure of 3D model quality) of each mesh generated using the above 5 setups for coin 003. Calculated using the Compute Geometric Measures filter in MeshLab version 2023.12.

	Setup 1	Setup 2	Setup 3	Setup 4	Setup 5
Avg Edge Length	0.006031	0.007358	0.014871	0.028886	0.020532

Table 3: The Control Scale Bar errors (as a measure of 3D model scale accuracy) for each of the 5 setups for coin 003.

Scaling Errors	Setup 1	Setup 2	Setup 3	Setup 4	Setup 5
Control bar 1	0.000123	0.000144	0.000140	0.000140	0.000144
Control bar 2	-0.000067	-0.000105	-0.000099	-0.000106	-0.000109
Control bar 3	-0.000057	-0.000041	-0.000043	-0.000035	-0.000036
Total (RMSE)	0.000087	0.000106	0.000102	0.000103	0.00106

Figure 14. A side-by-side comparison of the focus stacked (left) and pixel shifted (right) textured 3D models of coin 003, both generated from images taken with the Fujifilm GFX100s.

Figure 15. A side-by-side comparison of the focus stacked (left) and non-focus-stacked (right) textured 3D models of coin 003, both generated from images taken with the FujiFilm GFX100s.

Figure 16. A side-by-side comparison of the focus stacked (left) and non-focus-stacked (right) textured 3D models of coin 003, generated from images taken with the FujiFilm GFX100s (left) and Canon 5D MkIII (right).

Figure 17. A side-by-side comparison of the focus stacked (left) and non-focus-stacked (right) textured 3D models of coin 003, generated from images taken with the FujiFilm GFX100s (left) and Canon 7D MkII (right).

Figure 18. A side-by-side comparison of the focus stacked (left) and pixel shifted (right) untextured 3D models of coin 003, both generated from image sets taken with the Fujifilm GFX100s

Figure 19. A side-by-side comparison of the focus stacked (left) and non-focus-stacked (right) untextured 3D models of coin 003, both generated from images taken with the FujiFilm GFX100s.

Figure 20. A side-by-side comparison of the focus stacked (left) and non-focus-stacked (right) untextured 3D models of coin 003, generated from images taken with the FujiFilm GFX100s (left) and Canon 5D Mk III (right).

Figure 21. A side-by-side comparison of the focus-stacked (left) and non-focus-stacked (right) untextured 3D models of coin 003, generated from images taken with the FujiFilm GFX100s (left) and Canon 7D Mk II (right).

7. CONCLUSION

The integration of focus stacking with photogrammetry represents a significant advancement in the digitization of ancient coins and similar small artifacts. Through this integration, it is possible to capture the very delicate details of Roman coins with a level of quality that is unattainable using basic, non-focus-stacked photogrammetry methods, including the use of pixel-shifted super-resolution source images (e.g. obtained by using pixel-shifting). By addressing the limitations of conventional photogrammetry and incorporating an efficient workflow that leverages the automation and batch processing provided by modern photography hard- and software, it is possible to capture sub-millimeter details with an optimized and semi-automated workflow. Our focus stacking methodology has proven to be highly effective in achieving sub-millimeter detail in the digitized 3D models. Our integrated approach not only enhances the quality of the models but also makes the workflow more feasible for practical use in archaeological and cultural heritage projects. While it introduces overheads in terms of storage requirements, data transfer times, and extended processing durations—all significantly higher than the conventional non-focus-stacked methods for creating textured 3D models—the marked increase in detail and the overall quality of the final, textured 3D models justifies these additional resources. This advancement holds great promise for the fields of archaeology and cultural heritage, enabling more detailed and accurate documentation of artifacts and providing new insights into the past.

There is potential to achieve an even higher level of detail by increasing magnification even further and capturing a larger number of input images. However, due to time constraints, we were unable to extend the project's scope to explore these possibilities further. Future work could investigate the use of higher magnification, wider aperture settings, and a higher number of stacked images to push the limits of detail in photogrammetric digitization of objects of cultural heritage significance that require sub-millimeter levels of detail and quality. As technology continues to evolve, the continued refinement and application of these techniques will undoubtedly play a crucial role in preserving and understanding our shared history.

8. ACKNOWLEDGEMENTS

The authors would like to acknowledge Prof. Martin Smith of Bournemouth University's Archaeology and Anthropology department for his continued support and guidance.

9. REFERENCES

Abate, Francesco, Michela De Bernardin, Maria Stratigaki, et al. 2024. "X-Ray Computed Microtomography: A Non-Invasive and Time-Efficient Method for Identifying and Screening Roman Copper-Based Coins." Journal of Cultural Heritage 66: 436–43. https://doi.org/10.1016/j.culher.2023.12.008.

Adamopoulos, Efstathios, Fulvio Rinaudo, and Liliana Ardissono. 2021. "A Critical Comparison of 3D Digitization Techniques for Heritage Objects." ISPRS International Journal of Geo-Information 10 (1). https://doi.org/10.3390/ijgi10010010.

Antinozzi, Sara, Fausta Fiorillo, and Mirko Surdi. 2022. "Cuneiform Tablets Micro-Surveying in an

Optimized Photogrammetric Configuration." Heritage 5 (4): 3133–64. https://doi.org/10.3390/heritage5040162.

Armbruster, Barbara. 2023. "Fine Metalworking Tools and Workshops in Western and Northern Europe. A Diachronic Consideration." In Metalworkers and Their Tools. Symbolism, Function, and Technology in the Bronze and Iron Ages, edited by L. Boutoille and R. Peake. Archaeopress Archaeology.

Barszcz, Marcin, Jerzy Montusiewicz, Magdalena Paśnikowska-\Łukaszuk, and Anna Sa\łamacha. 2021. "Comparative Analysis of Digital Models of Objects of Cultural Heritage Obtained by the '3D SLS' and 'SfM' Methods." Applied Sciences 11 (12). https://doi.org/10.3390/app11125321.

Bentkowska-Kafel, Anna, Julio M. del Hoyo Melendez, Lindsay MacDonald, Aurore Mathys, and Vera Moitinho de Almeida. 2016. "Colour and Space in Cultural Heritage in 6Ds: The Interdisciplinary Connections." In CAA2015. Keep The Revolution Going: Proceedings of the 43rd Annual Conference on Computer Applications and Quantitative Methods in Archaeology, edited by Stefano Campana, Roberto Scopigno, and Gabriella Carpentiero. Archaeopress. https://doi.org/10.2307/jj.15135955.104.

Bentkowska-Kafel, Anna, Vera Moitinho de Almeida, Lindsay MacDonald, Julio M. del Hoyo Melendez, and Aurore Mathys. 2018. "Beyond Photography: An Interdisciplinary, Exploratory Case Study in the Recording and Examination of Roman Silver Coins." In Digital Techniques for Documenting and Preserving Cultural Heritage, edited by Anna Bentkowska-Kafel and Lindsay MacDonald. Arc Humanities Press. https://doi.org/10.2307/j.ctt1xp3w16.10.

Brecko, Jonathan, and Aurore Mathys. 2020. "Handbook of Best Practice and Standards for 2D+ and 3D Imaging of Natural History Collections." European Journal of Taxonomy 623. https://doi.org/10.5852/ejt.2020.623.

Bruun, Patrick. 1979. "The Successive Monetary Reforms of Diocletian." Museum Notes (American Numismatic Society) 24: 129–48.

Bruun, Patrick. 1997. "The Victorious Signs of Constantine: A Reappraisal." The Numismatic Chronicle 157: 41–59.

Cao, Frédéric, Frédéric Guichard, and Hervé Hornung. 2010. "Information Capacity: A Measure of Potential Image Quality of a Digital Camera." Digital Photography VI (Proc. SPIE 7537), 75370F. https://doi.org/10.1117/12.838903.

Clini, Paolo, Nicoletta Frapiccini, Maura Mengoni, Romina Nespeca, and Ludovico Ruggeri. 2016. "SfM Technique and Focus Stacking for Digital Documentation of Archaeological Artifacts." The International Archives of the Photogrammetry, Remote Sensing and Spatial Information Sciences XLI-B5: 229–36. https://doi.org/10.5194/isprs-archives-XLI-B5-229-2016.

DeSantis, Larisa R. G., Jessica R. Scott, Blaine W. Schubert, et al. 2013. "Direct Comparisons of 2D and 3D Dental Microwear Proxies in Extant Herbivorous and Carnivorous Mammals." PLOS ONE 8 (e71428). https://doi.org/10.1371/journal.pone.0071428.

Dey, Steven. 2018. "Potential and Limitations of 3D Digital Methods Applied to Ancient Cultural Heritage: Insights from a Professional 3D Practitioner." In Digital Imaging of Artefacts: Developments in Methods and Aims, edited by Kate Kelley and Rachel Wood. Archaeopress.

Đuric, Isidora, Ivana Vasiljevic, Miloš Obradovic, Vesna Stojakovic, Jelena Kicanovic, and Ratko Obradovic. 2021. "Comparative Analysis of Open-Source and Commercial Photogrammetry Software for Cultural Heritage." Proceedings of the 39th eCAADe Conference - Volume 2, 243–52.

https://doi.org/10.52842/conf.ecaade.2021.2.243.
D'Urso, Maria Grazia, and Joel Aldrighettoni. 2024. "Geodatabase, Metric Reconstruction and a GIS Platform of Historical-Archaeological Sites in Aquino." Acta IMEKO 13 (3): 1–14. https://doi.org/10.21014/actaimeko.v13i3.1779.
Falkingham, Peter L. 2020. "Photogrammetry: Does Shooting RAW or JPG Make a Difference?" https://peterfalkingham.com/2020/05/22/photogrammetry-does-shooting-raw-or-jpg-make-a-difference/.
Frakes, Robert M. 2005. "The Dynasty of Constantine Down to 363." In The Cambridge Companion to the Age of Constantine, edited by Noel Lenski. Cambridge University Press.
Gajski, Dubravko, Ana Solter, and Mateo Gašparovic. 2016. "Applications of Macro Photogrammetry in Archaeology." The International Archives of the Photogrammetry, Remote Sensing and Spatial Information Sciences XLI-B5: 263–66. https://doi.org/10.5194/isprs-archives-XLI-B5-263-2016.
Galantucci, Luigi Maria, Maria Grazia Guerra, and Fulvio Lavecchia. 2018. "Photogrammetry Applied to Small and Micro Scaled Objects: A Review." In Proceedings of AMP 2018: 3rd International Conference on the Industry 4.0 Model for Advanced Manufacturing. https://doi.org/10.1007/978-3-319-89563-5_4.
Gallo, Alessandro, Fabio Bruno, Maurizio Muzzupappa, and Mauro F. La Russa. 2012. "Multi-View 3D Reconstruction of Small Stone Samples Deteriorated by Marine Organisms." 18th International Conference on Virtual Systems and Multimedia, 181–87. https://doi.org/10.1109/VSMM.2012.6365923.
Gallo, Alessandro, Maurizio Muzzupappa, and Fabio Bruno. 2014. "3D Reconstruction of Small Sized Objects from a Sequence of Multi-Focused Images." Journal of Cultural Heritage 15 (2): 173–82. https://doi.org/10.1016/j.culher.2013.04.009.
García-Bustos, Miguel, Xabier Eguilleor-Carmona, Olivia Rivero, and Ana María Mateo-Pellitero. 2024. "3D Recording of Palaeolithic Rock Art through Different Techniques: A Critical Comparison and Evaluation." Journal of Field Archaeology 49 (7): 508–26. https://doi.org/10.1080/00934690.2024.2392972.
Gillies, David. 2015. "Close Range Photogrammetry." The Photogrammetric Record 30: 318–22. https://doi.org/10.1111/phor.12114.
Gołyźniak, Paweł. 2020. Engraved Gems and Propaganda in the Roman Republic and under Augustus. Vol. 65. Roman Archaeology. Archaeopress.
Guidi, Gabriele, Umair Shafqat Malik, and Laura Loredana Micoli. 2020. "Optimal Lateral Displacement in Automatic Close-Range Photogrammetry." Sensors 20 (21). https://doi.org/10.3390/s20216280.
Hernández-Muñoz, Óscar. 2023. "Analysis of Digitized 3D Models Published by Archaeological Museums." Heritage 6 (5): 3885–902. https://doi.org/10.3390/heritage6050206.
Hess, Mona, Lindsay W. MacDonald, and Jaroslav Valach. 2018. "Application of Multi-Modal 2D and 3D Imaging and Analytical Techniques to Document and Examine Coins on the Example of Two Roman Silver Denarii." Heritage Science 6: 1–22.
Historic England. 2017. Photogrammetric Applications for Cultural Heritage: Guidance for Good Practice. Historic England.
Kampel, Martin, Sebastian Zambanini, Mario Schlapke, and Bernd Breuckmann. 2009. "Highly Detailed 3D Scanning of Ancient Coins." 22nd CIPA Symposium.

Kemmers, Fleur, and Nanouschka Myrberg. 2011. "Rethinking Numismatics. The Archaeology of Coins." Archaeological Dialogues 18 (1): 87–108. https://doi.org/10.1017/S1380203811000146.
Kingsland, Kaitlyn. 2020. "Comparative Analysis of Digital Photogrammetry Software for Cultural Heritage." Digital Applications in Archaeology and Cultural Heritage 18: e00157. https://doi.org/10.1016/j.daach.2020.e00157.
Kontogianni, Georgia, Regina Chliverou, Anestis Koutsoudis, George Pavlidis, and Andreas Georgopoulos. 2017. "Enhancing Close-Up Image Based 3D Digitisation with Focus Stacking." The International Archives of the Photogrammetry, Remote Sensing and Spatial Information Sciences XLII-2/W5: 421–25. https://doi.org/10.5194/isprs-archives-XLII-2-W5-421-2017.
Kropff, Antony. 2017. "Diocletian's Currency System After 1 September 301: An Inquiry Into Values." Revue Belge de Numismatique et de Sigillographie 163: 167–87. http://www.numisbel.be/2017_6.pdf.
Lastilla, Lorenzo, Roberta Ravanelli, Miguel Valério, and Silvia Ferrara. 2021. "Modelling the Rongorongo Tablets: A New Transcription of the Échancrée Tablet and the Foundation for Decipherment Attempts." Digital Scholarship in the Humanities 37 (2): 497–516. https://doi.org/10.1093/llc/fqab045.
MacDonald, Lindsay, Vera Moitinho de Almeida, and Mona Hess. 2017. "Three-Dimensional Reconstruction of Roman Coins from Photometric Image Sets." Journal of Electronic Imaging 26 (1): 011017. https://doi.org/10.1117/1.JEI.26.1.011017.
Marziali, Stefano, and Giulia Dionisio. 2017. "Photogrammetry and Macro Photography. The Experience of the MUSINT II Project in the 3D Digitizing Process of Small Size Archaeological Artifacts." Studies in Digital Heritage 1 (2): 298–309. https://doi.org/10.14434/sdh.v1i2.23250.
Mattingly, Harold. 1946. "The Monetary Systems of the Roman Empire from Diocletian to Theodosius I." The Numismatic Chronicle and Journal of the Royal Numismatic Society 6 (3/4): 111–20.
Morris, Gala, Joshua Emmitt, and Jeremy Armstrong. 2022. "Depth and Dimension: Exploring the Problems and Potential of Photogrammetric Models for Ancient Coins." Journal of Computer Applications in Archaeology 5 (1): 112–22. https://doi.org/10.5334/jcaa.99.
Mosbrucker, Adam R., Jon J. Major, Kurt R. Spicer, and John Pitlick. 2017. "Camera System Considerations for Geomorphic Applications of SfM Photogrammetry." Earth Surface Processes and Landforms 42: 969–86. https://doi.org/10.1002/esp.4066.
Nicols, John. 2007. "Mapping the Crisis of the Third Century." In Crises and the Roman Empire, edited by Olivier Hekster, Gerrit de Kleijn, and Daniëlle Slootjes. Brill.
O'Connor, James. 2018. "Impact of Image Quality on SfM Photogrammetry: Colour, Compression and Noise." PhD Thesis, Kingston University.
Olkowicz, Marcin, Marcin Dabrowski, and Anne Pluymakers. 2019. "Focus Stacking Photogrammetry for Micro-Scale Roughness Reconstruction: A Methodological Study." The Photogrammetric Record 34 (165): 11–35. https://doi.org/10.1111/phor.12270.
Percoco, Gianluca, Maria Grazia Guerra, Antonio Jose Sanchez Salmeron, and Luigi Maria Galantucci. 2017. "Experimental Investigation on Camera Calibration for 3D Photogrammetric Scanning of Micro-Features for Micrometric Resolution." International Journal of Advanced Manufacturing Technology 91: 2935–47. https://doi.org/10.1007/s00170-016-9949-6.
Piazza, Amedeo, Sergio Corvino, Daniel Ballesteros, et al. 2024. "Neuroanatomical Photogrammetric

Models Using Smartphones: A Comparison of Apps." Acta Neurochirurgica 166: 378. https://doi.org/10.1007/s00701-024-06264-y.
Plisson, Hugues, and Lydia V. Zotkina. 2015. "From 2D to 3D at Macro- and Microscopic Scale in Rock Art Studies." Digital Applications in Archaeology and Cultural Heritage 2 (2–3): 102–19. https://doi.org/10.1016/j.daach.2015.06.002.
Polo, María-Eugenia, Ángel M. Felicísimo, and Guadalupe Durán-Domínguez. 2022. "Accurate 3D Models in Both Geometry and Texture: An Archaeological Application." Digital Applications in Archaeology and Cultural Heritage 27: e00248. https://doi.org/10.1016/j.daach.2022.e00248.
Qian, Guocheng, Yuanhao Wang, Jinjin Gu, Chao Dong, Wolfgang Heidrich, and Bernard Ghanem. 2022. "Rethinking Learning-Based Demosaicing, Denoising, and Super-Resolution Pipeline." 2022 IEEE International Conference on Computational Photography (ICCP), 1–12. https://doi.org/10.1109/ICCP54855.2022.9887682.
Ravanelli, Roberta, Lorenzo Lastilla, and Silvia Ferrara. 2022. "A High-Resolution Photogrammetric Workflow Based on Focus Stacking for the 3D Modeling of Small Aegean Inscriptions." Journal of Cultural Heritage 54: 130–45. https://doi.org/10.1016/j.culher.2022.01.009.
Redford, Adam, Richard Mikulski, and Eike Falk Anderson. 2020. "Streamlining Photogrammetry Reconstructions of Bone Fragments for Bioarchaeological Analysis, Conservation, and Public Engagement." Eurographics 2020 Posters. https://doi.org/10.2312/egp.20201036.
Saif, Wahib, and Adel Alshibani. 2022. "Smartphone-Based Photogrammetry Assessment in Comparison with a Compact Camera for Construction Management Applications." Applied Sciences 12 (3). https://doi.org/10.3390/app12031053.
Scaggion, Cinzia, Stefano Castelli, Donatella Usai, and Gilberto Artioli. 2022. "3D Digital Dental Models' Accuracy for Anthropological Study: Comparing Close-Range Photogrammetry to µ-CT Scanning." Digital Applications in Archaeology and Cultural Heritage 27: e00245. https://doi.org/10.1016/j.daach.2022.e00245.
Schirripa Spagnolo, Giuseppe, Lorenzo Cozzella, and Fabio Leccese. 2021. "Fringe Projection Profilometry for Recovering 2.5D Shape of Ancient Coins." Acta IMEKO 10 (1): 142–49. https://doi.org/10.21014/acta_imeko.v10i1.872.
Schirripa Spagnolo, Giuseppe, Raffaele Majo, Marco Carli, Dario Ambrosini, and Domenica Paoletti. 2003. "Virtual Gallery of Ancient Coins through Conoscopic Holography." Optical Metrology for Arts and Multimedia (Proc. SPIE 5146), 202–9. https://doi.org/10.1117/12.500589.
Stamatopoulos, Christos, Clive S. Fraser, and Simon Cronk. 2012. "Accuracy Aspects of Utilizing Raw Imagery in Photogrammetric Measurement." The International Archives of the Photogrammetry, Remote Sensing and Spatial Information Sciences XXXIX-B5: 387–92. https://doi.org/10.5194/isprsarchives-XXXIX-B5-387-2012.
Stevenson, Seth William, Charles Roach Smith, and Frederic William Madden. 1889. A Dictionary of Roman Coins, Republican and Imperial. G. Bell and Sons.
Tolksdorf, Johann Friedrich, Rengert Elburg, and Thomas Reuter. 2017. "Can 3D Scanning of Countermarks on Roman Coins Help to Reconstruct the Movement of Varus and His Legions." Journal of Archaeological Science: Reports 11: 400–410. https://doi.org/10.1016/j.jasrep.2016.12.005.
Zambanini, Sebastian, Mario Schlapke, Michael Hödlmoser, and Martin Kampel. 2010. "3D Acquisition of Historical Coins and Its Application Area in Numismatics." Computer Vision and Image Analysis of Art (Proc. SPIE 7531). https://doi.org/10.1117/12.840203.

Zambanini, Sebastian, Mario Schlapke, Martin Kampel, and Andreas Müller. 2009. “Historical Coins in 3D: Acquisition and Numismatic Applications.” VAST 2009: The 10th International Symposium on Virtual Reality, Archaeology and Cultural Heritage, Short & Project Papers.

10. APPENDICES

10.1 Appendix 1 – Powershell script for moving files into folders for focus stacking:

```
# Define the source folder containing the files
$sourceFolder = "C:\Path\To\Your\SourceFolder"

# Get the list of files in the source folder, sorted by name
$files = Get-ChildItem -Path $sourceFolder | Sort-Object Name

# Define the destination folder where the new folders will be created
$destinationFolder = "C:\Path\To\Your\DestinationFolder"

# Create the destination folder if it doesn't exist
if (-Not (Test-Path -Path $destinationFolder)) {
   New-Item -ItemType Directory -Path $destinationFolder
}

# Initialize variables for folder and file counting
$folderCount = 1
$fileCount = 0

# Loop through each file and move it to the appropriate folder
foreach ($file in $files) {
   # Calculate the current folder name
   $currentFolder = "$destinationFolder\00$folderCount"

   # Create the current folder if it doesn't exist
   if (-Not (Test-Path -Path $currentFolder)) {
      New-Item -ItemType Directory -Path $currentFolder
   }

   # Move the file to the current folder
   Move-Item -Path $file.FullName -Destination $currentFolder

   # Increment the file count
   $fileCount++
```

```
    # If the required number of files have been moved to the current folder, reset the file count and
      move to the next folder
    if ($fileCount -eq insertNumberOfImagesPerStackHere) {
        $fileCount = 0
        $folderCount++
    }
}

Write-Host "Files have been folderized."
```

10.2 Appendix 2 – Links to the final textured 3D models on SketchFab.

RomanCoin_001: -
https://sketchfab.com/3d-models/romancoin-001-16d8c98e91de4b18b7e9bb601d55d187
RomanCoin_002: –
https://sketchfab.com/3d-models/romancoin-002-02df34af4ed94db2a85857a155b3e68d
RomanCoin_003: –
https://sketchfab.com/3d-models/romancoin-003-109c6b66e3084707a7fafa2056f41562
RomanCoin_004: –
https://sketchfab.com/3d-models/romancoin-004-e98df75d8dc2417ba8df7f1bdb5ddc81

Received November 2024; revised June 2025; accepted November 2025.